PCCP

Accepted Manuscript

ROYAL SOCIETY OF CHEMISTRY

www.rsc.org/pccp

Band gap engineering of early transition-metal-doped anatase TiO_2: First principle calculations

C. Li[1]*, Y. F. Zhao[1], Y. Y. Gong[1], T. Wang[2]*, and C. Q. Sun[1,3],

[1] Center for Coordination Bond Engineering, School of Materials Science and Engineering, China Jiliang University, China

[2] College of Electrical Engineering, Zhejiang University, China

[3] School of Electrical and Electronic Engineering, Nanyang Technological University, Singapore

E-mail: canli1983@gmail.com; twang@zju.edu.cn

Abstract

The thermal stability and electronic structures of anatase TiO_2 doped by early transition metals (TM) (III-B group = Sc, Y and La; IV-B group = Zr and Hf; V-B group = V, Nb and Ta) have been studied using first principle calculations. It was found that all doped systems are thermodynamically stable, and their band gaps were reduced by 1~1.3 eV compared with pure TiO_2. Doping by transition metals affects the strength of hybrid orbital of TM-O bonding, and the band gap increases approximately linearly with the MP value of TM-O bonding.

Keywords: doped anatase TiO_2, early transition metals, band gap, and chemical bond.

I. INTRODUCTION

In recent decades, titania (TiO_2) has drawn great interest as a promising material for catalytic and photochemical applications.[1-3] However, its low reaction efficiency still remains a main challenge preventing the widely practical applications.[4, 5] It is known that TiO_2 is a wide band gap semiconductor (E_g = 3.20 eV for anatase phase and 3.00 eV for rutile phase),[6-9] and thus can only be excited by UV light irradiation, i.e. only about ~5% of solar spectrum can be absorbed by TiO_2. Therefore, it is of great importance to extend the optical absorption region of TiO_2-based photocatalysts to the visible and/or near infrared spectral range.[10, 11]

It has been proposed previously that doping can adjust the band gap and extend the optical absorption edge toward the longer wavelength.[12, 13] Up to now, various research groups have investigated doping TiO_2 by transition metals (TM)[14, 15] and/or non-metals. [16, 17] It was found that the lattice structure of TiO_2 is distorted by the incorporation of TM dopants, such as Fe, Co, Mo, Nb and V,[18-21] which results in the red shift of the absorption edge and decreases the recombination rate of photogenerated carriers. One the other hand, doping by non-metal dopants, such as N, C S and Sn,[10, 12, 13, 16, 22, 23] shifts the top of valence band to higher energies, and thus reduces the forbidden band gap. Moreover, the optical and photocatalytic properties can be further improved by co-doping: doped by more than one type of dopant, such as TM and non-metal,[24-27] non-metal and non-metal[28] as well as non-metal and hydrogen doping.[29-31] The co-doped systems exhibit enhanced photocatalytic efficiency compared with the mono-doped TiO_2 photocatalysts.

Although the optical properties of several doped TiO_2 systems have been studied up to now, the understanding of the chemical bond between dopant and O (or Ti) is ambivalent, which is critical to improve the optical performance of TiO_2-based photocatalysts.[32] Dopants in TiO_2 will change the bond energy, electronic structure and iconicity (the ratio of ionic bonding part in chemical bond[33, 34]), as well as the electronic distribution of chemical bond. Thus, a detailed study of the chemical bond between different types of dopants and O (or Ti) is necessary to understand the fundamental mechanism of chemical bonds in doped TiO_2.

In this work, the first principle calculations were carried out on anatase TiO_2 systems doped by early TM (III-B group = Sc, Y and La; IV-B group = Zr and Hf; V-B group = V, Nb and Ta). The crystal and electronic structures, as well as thermal stability are simulated, and the effects of different kinds of dopants on electronic structures and chemical bond of TM-O bonding were compared.

II. Computational Method

The doped anatase TiO_2 with space group $I4_1$/amd (see Fig. 1a) symmetry was studied. The first principle simulations were used to calculate the crystal structure, formation energy, partial density of states (PDOS), electron density difference diagrams, band structures, Mulliken charge (MC) and Mulliken bond population (MP). The calculations were based on density functional theory with the Perdew-Burke-Ernzerhof functional of the generalized gradient approximation (GGA) [35] and norm-conserving pseudopotentials,[36] as implemented in the CASTEP package. 2*2*1 super-cell with $TMTi_{15}O_{32}$ was built where the TM element substitutes Ti atom (see Fig. 1a). The cutoff kinetic energy of electron wave function was 750 eV, which is sufficiently large for the systems considered. The *k*-point sampling set 5×5×4 division of the reciprocal unit cell based on the Monkhorst-Pack[37] scheme was found to be converged. The convergence tolerance of energy, maximum force, and maximum displacement is 5.0×10^{-6} eV/atom, 0.01 eV/Å, and 5.0×10^{-4} Å, respectively. The MC and MP are calculated according to the formalism described by Segall et al.[38, 39] A linear combination of atomic orbitals (LCAO) basis set was used to provide a natural way of specifying quantities such as atomic charge, bond population and charge transfer, and the overlap population is used to assess the covalent or ionic nature of a bond. [38] The GGA+U approach, which introduces an intra-atomic electron–electron interaction as an on-site correction to describe systems with localized *d* and *f* states, can produce more precise band gap than GGA. [40-42] To account for the strongly correlated interactions among the Ti 3*d* electrons and calculate the electronic structures, a moderate on-site Coulomb repulsion U = 7.0 eV was applied. The calculated band gap is 3.18 eV, which is close to the experimental

value of 3.20 eV. The relationship between U values and band gaps of anatase TiO_2 was shown in Fig. 1b.

To investigate the thermal stability of TM doped in an anatase TiO_2 host, it is useful to define the substitution energy of TM impurity as:

$$E_s = E(TMTi_{15}O_{32}) + E(Ti) - E(TM) - E(Ti_{16}O_{32}) \quad (1)$$

where $E(TMTi_{15}O_{32})$ and $E(Ti_{16}O_{32})$ are the total energy of doped and pure super-cell anatase TiO_2, respectively; E(Ti) and E(TM) are energy per atom for the elemental Ti and TM impurity, respectively (see Tab. 1).

Meanwhile, the formation energy of pure TiO_2 was calculated as:

$$E_f = E(Ti_{16}O_{32}) - 16*E(Ti) - 32*E(O) \quad (2)$$

where E(O) is the energy per atom in O_2 gas.

III. Results and Discussion

Lattice constant and substitution energy

The lattice constants of all doped systems studied in this work were calculated and listed in Tab. 1. It is found that the calculated a of all the doped systems are larger than that of pure TiO_2 except for V-doped TiO_2, while the calculated c of the systems doped by III-B and IV-B elements (V-B elements) are larger (smaller) than that of pure TiO_2. Although doping by foreign elements results in the variation of lattice constants, the deformations of a and c are less than 0.1% except La-doped TiO_2 which exhibits up to 3.4% deformation in c axis. So these doped systems are structural stable. Our calculated results of pure TiO_2 are $a = b$ =7.564 Å and c = 9.564 Å, which is in excellent agreement with the previously reported experimental values ($a = b$ = 7.568 Å, c = 9.515 Å)[43] and calculated values (a = b = 7.552 Å, c = 9.486 Å).[44]

Moreover, the substitution energies of all the doped systems were calculated by Eq. 1 and the results are listed in Tab. 1. The substitution energy of Zr or Hf (IV-B group element)-doped TiO_2 show negative values, and thus are more stable than pure TiO_2, whereas III-B or V-B group element-doped TiO_2 show positive values and thus are less stable than pure TiO_2, indicating that III-B or V-B group element doped TiO_2 is more difficult to synthesize than pure TiO_2. However, compared with the formation

energy (E_f) of -164.37 eV for pure TiO_2 calculated by Eq. 2, the values of E_s of all doped systems is less than 2.5% of E_f, and equals to -430.85 eV, -7.90 eV, -4.38 eV for $E(Ti_{16}O_{32})$, E(Ti) and E(O), respectively. Thus, all doped systems are thermodynamically stable.

Band structure and PDOS

The band structures of all the systems were calculated and plotted in Fig .2, and the extracted band gaps were listed in Tab. 1, which are comparable with the previously reported values obtained by first principal calculations[19, 44-48] and experimental observations [49-52] (see Tab. 1). The band gaps of all the doped systems were reduced by 1.0~1.3 eV, compared with that of pure TiO_2, which then lead to the red shift of the optical absorption edge and visible light could be absorbed by doped systems. Similar phenomena have been found by other groups both theoretically and experimentally.[24, 45, 49, 51] Moreover, the level of decrease of the band gap depends on the position of dopants in the periodic table, i.e. for dopants in III-B group, E_g reduces as the atomic number of the dopant increases; whereas, E_g increases as the atomic number of the dopant increases for dopants from IV-B and V-B groups.

The reasons of the reduction in the band gap of the doped systems were analyzed based on their conduct and valent orbitals, and the PDOS of all systems were calculated. Since the PDOS of doped systems are homologous for dopants lie in the same group, only three doped systems, i.e. Y-, Zr- and Nb-doped systems, were list as example, and the calculated results were compared with that of pure TiO_2, see Fig. 3. As shown in Fig. 3a, the valence band are mainly made up of O-2*p*, Ti-4p and -3*d* orbital and the conduce band are mainly made up of O-2*p* and Ti-3*d* orbital for pure TiO_2. Meanwhile, O-2*p* orbital hybrid with Ti-4p and -3*d* orbital between 0 ~ -5.0 eV in valent band; and O-2*p* orbital hybrid with Ti -3*d* orbital hybrid between 3.3 ~ 5.5 eV in conduct band. The PDOS of pure TiO_2 is the same as the other's result.[53] Figs. 3b, 3c and 3d plot the *s*, *p* and *d* orbital of the dopant atom and *p* orbital of one O atom for Y-, Zr-, and Nb-doped TiO2, respectively. For Y-doped TiO_2, Y-5*p* and -4*d* orbital hybrid with O-2*p* orbital between 0 ~ -4.8 eV in valent band, and the valence band moves towards the Fermi level (E_F), which then in turn lead to the shift of

conduction band towards E_F, resulting in the reducing of band gap. Similar tendency is observed in Zr doped systems. However, Nb-doped TiO_2 behave differently. When Nb atom was introduced to TiO_2, Nb -5*p* and -4*d* orbital hybrid with O-2*p* orbital between -7.8 ~ -2.3 eV in valence band and Nb-4*d* orbital hybrid with the O-2*p* orbital between 0 ~ 2.1 eV in conduce band. The shift of both valence and conduce band toward left relative to the E_F indicates that the E_F moved towards high energy level (from valence band maximum to conduce band minimum compared pure TiO_2) after Nb atom was doped, which may be caused by the extra one valence electron of V-B group elements than Ti.

Since the reduction in the band gap was due to the shift of valence band and conduce band, to estimate the moving distance, the valence band center $\tilde{N}$, denotes as the average energy of valence electrons, is calculated and the results are given in Tab. 1. It is found that the valence band center moved toward the E_F about 0.2 eV for III-B and VI-B group element-doped systems and conduce band moved about 0.8 eV since the occupied orbital in valence band (about 258) is four times the unoccupied orbital in conduce band (about 66) by integrating the area of valence band and conduce band of total DOS individually. Thus, the total moving distance of valence band and conduce band is about 1.0 eV, which is approximately equals to the value of the reduction in the band gap, and the small difference may be caused by the widening of the conduce band. For example, the width of conduce band is 2.2 eV and 2.5 eV for pure TiO_2, and Y- (or Zr-) doped systems (calculated form Fig. 3a, 3b and 3c), respectively. Although the absolute value $\tilde{N}$ of V-B group element-doped system is meaningless since the E_F of them were moved, the higher the value of $\tilde{N}$, the smaller the value of band gap. Therefore, the moving of valence band and conduce band reduces band gap of V-, Nb- or Ta- doped systems.

Mulliken charge and bond population

The trends of band gap reduction were analyzed for dopants in different groups, and the MC of all systems were calculated and the obtained results are shown in Fig. 4a and Tab. 1. Two different trends are observed for dopants from different groups, i.e., MC decreases as the atomic number of dopant decreases for elements in III-B

group including La, Y, and Sc, while MC increases as the atomic number of dopant decreases for elements in VI-B groups from Hf to Zr (VI-B group) and elements from V-B groups including Ta, Nb, and V. For dopant in the same group, the value of MC is approximately inversely proportional to band gap. As mentioned previously, the variation of the band gap was caused by the hybrid orbital, and thus the larger value of transferring charge (MC) and the stronger the hybrid orbital lead to the smaller band gap of the doped TiO_2 for dopants in the same group. Although the band gap of the doped system is related with the value of MC for dopant in the same group, the absolute values of MC are meaningless since the numbers of valence electrons are different for dopant from different group.

To found the consistent changing trend of band gap for dopants lie in different group, the MP of TM-O bonding of all the systems were calculated and the obtained results are shown in Fig. 4b and Tab. 1 since band gap of insulator or semiconductor is decided by its chemical bond which includes the ionic bonding and covalent bonding. Several papers have reported previously that the overlap population can be used to assess the covalent or ionic nature of a bond.[34, 54] Since a high value of MP correspond to a high percentage of covalent bonding for materials with the same crystal structure and symmetry,[34] the values of MP denote the strength of hybrid orbital in each chemical bond which is related to the band gap. Considering the same structure and symmetry for all the doped and un-doped systems, they have the same the MP value, about 0.38, for chemical bond Ti-O, whereas it is likely that the value of band gaps in doped systems may be related to the MP values of TM-O bonding, and the calculated results are listed in Tab. 1 and plotted in Fig. 4b. It is found that the MP values of TM-O bonding are changed for different doped systems. Specifically, MP is inversely proportional to MC for dopant in the same group (see Figs 4a and 4b), and an approximate linear relationship is found between the MP values and band gaps of all the doped systems, particularly for dopants lied in V-B group. Thus, the band gap of doped TiO_2 system is decided directly by the TM-O bonding.

Therefore, the strength of hybrid orbital of chemical bond determines the band gap of TM-doped TiO_2. For dopants lie in the same group, the more the transferring

charge (MC) and the stronger the hybrid orbital, the smaller the band gap. Moreover, the MP value is related to the strength of hybrid orbital in chemical bond directly, and the band gap of the TM-doped system increases approximately linearly with MP.

IV. CONCLUSIONS

In summary, the anatase TiO_2 systems doped by elements belonging to III-B, IV-B and V-B groups were studied by first principles calculations. The effects of different dopants on the electronic structure and chemical bond of TM-O were investigated in detail. It was found that all the doped systems are thermodynamically stable, and the band gaps of all doped systems were reduced by 1~1.3 eV compared with pure TiO_2. Doping by transition metals affects the strength of hybrid orbital of TM-O bonding, and the band gap increases approximately linearly with the MP value of TM-O bonding.

ACKNOWLEDGEMENTS

Computational resources have been provided by the Beijing Computing Center.

References

1 S. U. M. Khan, M. A. Shahry, and W. B. I. Jr, Science **297**, 2243 (2002).

2 X. Chen, L. Liu, P. Y. Yu, and S. S. Mao, Science **331**, 746 (2011).

3 L. Schmidt-Mende, J. K. Stolarczyk, and S. N. Habisreutinger, Angew. Chem. Int. Ed. **52**, 7372 (2013).

4 C. Das, P. Roy, M. Yang, H. Jha, and P. Schmuki, Nanoscale **3**, 3094 (2011).

5 G. C. F. Spadavecchia, S. Ardizzone, M. Ceotto, and L. Falciola, J. Phys. Chem. C **115**, 6381 (2011).

6 U. Diebold, Surf. Sci. Rep. **48(5-8)** (2003).

7 X. J. Liu, L. K. P., Z. Sun, Y.M. Chen, X.X. Yang, L.W. Yang, Z.F. Zhou, and C.Q. Sun , J. Appl. Phys **110(4)**, 044322 (2011).

8 D. Lee and Y. Kanai, J. Am. Chem. Soc. **134**, 20266 (2012).

9 D. Tsukamoto, Y. S., Y. Sugano, S. Ichikawa, S. Tanaka and T. Hirai, J. Am. Chem. Soc. **134**, 6309 (2012).

10 X. P. Han and G. S. Shao, J. Phys. Chem. C **115**, 8274 (2011).

11 T. Xia, N. L., Y. L. Zhang, M. B. Kruger, J. Murowchick, A. Selloni and X. B. Chen, ACS Appl. Mater. Inter. **5**, 9883 (2013).

12 J .Wang, N. T., J. P. Lewis, et al., J. Am. Chem. Soc. **131**, 12290 (2009).

13 D. Q. Zhao, X. W. H., B. L. Tian, S. M. Zhou, Y. C Li, and Z. L. Du Appl. Phys. Lett. **98**, 162107 (2011).

14 Z. Y. Zhao, Z. S. L., and Z. G. Zou, Chem. Phys. Chem. **13**, 3836 (2012).

15 X. H. Yu, T. J. H., X. H. Sun, and Y. Y. Li, Chem. Phys. Chem. **13**, 1514 (2012).

16 M. Harb, P. S., and P. Raybaud, J. Phys. Chem. C **117**, 8892 (2013).

17 M. Khan, J. N. X., N. Chen, and W. B. Cao, J. Alloy. Compd. **513**, 539 (2012).

18 H. M. Weng, X. P. Y., J. M. Dong, H. Mizuseki, M. Kawasaki, and Y. Kawazoe, Phys. Rev. B **69**, 125219 (2004).

19 X. S. Du, Q. X. L., H. B. Su, and J. L. Yang, Phys. Rev. B **74**, 233201 (2006).

20 L. H. Gan, C. C. W., Y. Tan, et al., J. Alloy. Compd. **585**, 729 (2014).

21 Y. Li, Y. Y., Z.-Q. Que, M. Zhang, and M. Guo, Int. J. Min. Met. Mater. **20**,

1012 (2013).

22 W J. Zhang, W. F., J. H. Xi, *et al*., J. Alloy. Compd. **575**, 40 (2013).

23 J. Li and H. C. Zeng, J. Am. Chem. Soc **129**, 15839 (2007).

24 R. Long, and N. J. English, Chem. Phys. Lett. **478**, 175 (2009).

25 S. S. Liu, Q. L., C. C. Hou, X. D. Feng and Z. S. Guan. J. Alloy. Compd. **575**, 128 (2013).

26 M. Y. Xing, Y. M. W., J. L. Zhang and F. Chen, Nanoscale **2**, 1233 (2010).

27 X. P. Cao, D. L., W. H. Jing, W. H. Xing and Y. Q. Fan, J. Mater. Chem. **22**, 15309 (2012).

28 K. S. Yang, Y. D., and B. B. Huang, J. Phys. Chem. C **111**, 18985 (2007).

29 M. Li, J. Y. Z., D. Guo, and Y. Zhang, Chem. Phys. Lett. **539-540**, 175 (2012).

30 H. Pan, Y. W. Z., V. B. Shenoy, and H. J. Gao, J. Phys. Chem. C **115**, 12224 (2011).

31 L. Mi, P. Xu, H. Shen and P.-N. Wang, Appl. Phys. Lett **90**, 171909 (2007).

32 C. Q. Sun, Heidelberg New York Dordrecht London Singapore 805 **108** (2014).

33 J. C. Phillips, Rev. Mod. Phys. **42**, 317 (1970).

34 J .L. He, E. D. W., H. T. Wang, R. P. Liu and Y.J. Tian, Phys. Rev. Lett. **94**, 015504 (2005).

35 J. P. Perdew, K. B., and M. Ernzerhof, Phys. Rev. Lett. **77**, 3865 (1996).

36 D. R. Hamann, M. S., and C. Chiang, Phys. Rev. Lett. **43**, 1494 (1979).

37 H. J. Monkhorst and J. D. Pack, Phys. Rev. B **13**, 5188 (1976).

38 M. D. Segall, C. J. Pickard, R. Shah, and M. C. Payne, Mol. Phys. **89**, 571 (1996).

39 M. D. Segall, R. Shah, C. J. Pickard, and M. C. Payne, Phys. Rev. B **54**, 16317 (1996).

40 V. I. Anisimov, J. Zaanen and O. K. Andersen, Phys. Rev. B **44**, 943 (1991).

41 C. Li, J. S. Lian, and Q. Jiang, Phys. Rev. B **83**, 235125 (2011).

42 C. Li, J. C. L., J. S. Lian, and Q. Jiang,, J. Appl. Phys. **106**, 094102 (2009).

[43] M. Horn, C. F. S., E.P. Meagher, Z. Kristallogr, Zeitschrift Fur Kristallographie **136**, 273 (1972).

[44] J. G. Yu, P. Zhou, and Q. Li, Phys. Chem. Chem. Phys. **15**, 12040-12047 (2013).

[45] H. Kamisaka, T. H. T. Suenaga, T. Hasegawa, and K. Yamashita, J. Chem. Phys. **131**, 034702 (2009).

[46] X. J. Yao, X. D. W., L. Su, H. Yan and M. Yao, J. Mol. Catal. A-Chem. **351**, 11 (2011).

[47] A. Stashans and Y. Bravo, Mod. Phys. Lett. B **27**, 1350113 (2013).

[48] Y. Q. Wang, R. R. Zhang, J. B. Li, L. L. Li and S. W. Lin, Nanoscale. Res. Lett. **9**, 46 (2014).

[49] D. D. Mulmi, T. Sekiya, N. Kamiya, S. Kurita, Y. Murakami, T. Kodaira, J. Phys. Chem. Solids, **65**, 1181 (2004).

[50] M. Khan, Y. Song, N. Chen, W. Cao, Mater.s Chem. Phys. **142**, 148 (2013).

[51] K. M. Rahulan, L. D. Stephen, C. C. Kanakam, Appl. Surf. Sci. **266**, 326 (2013).

[52] P.C. Ricci, C.M. Carbonaro, A. Geddo Lehmann, F. Congiu, B. Puxeddu, G. Cappelletti, F. Spadavecchia, J. Alloy. Comp. **561**, 109 (2013).

[53] D. O. Scanlon, C. W. Dunnill, J. Buckeridge, et al., Nat. Mater. **12**, 798 (2013).

[54] C. Li, J.C. Li and Q. Jiang, Solid. State. Comm. **150**, 1818 (2010).

Captions:

Fig. 1. (Color online) (a) anatase TiO_2 doped by transition metals, where red, gray, and blue denotes oxygen, titanium, and dopant atoms, respectively; (b) the relationship between U values and band gaps of anatase TiO_2, and U = 7eV has been used. The calculated band gap E_g = 3.18 eV approximately equals to the experimental value of 3.20 eV.

Fig. 2. (Color online) Band structures of pure TiO_2 and doped systems. Band gaps of all the doped systems reduced by 1.0 ~ 1.3 eV compared with that of pure TiO_2.

Fig. 3. (Color online) The PDOS of (a) pure TiO_2, (b) Y-doped TiO_2, (c) Zr-doped TiO_2 and (d) Nb-doped TiO_2. The illustrations display the corresponding comparison between the *s*, *p* and *d* orbital of one dopant atom and *p* orbital of one O atom. The PDOS of Y and Zr doped TiO_2 have similar results and different from that of Nb doped TiO_2.

Fig. 4. (Color online) The relationships between MC values (a), MP values (b) and E_g of all doped systems. E_g increases approximately linearly with MP values.

Table 1. The equilibrium lattice constants a, b and c with unit Å, the total energy of doped systems E^{sys}, energy per atom for the elemental TM E_{TM}, substitution energy of transition metals impurity E_s with unit eV; the valence band center $\tilde{N}$ with unit eV; the band gap estimated in this work E_g, the previously reported band gap obtained by simulation E'_g and experimental measurements E''_g with unit eV; MC and MP values of all considered systems.

Dopant	$a = b$	c	E^{sys}	E_{TM}	E_s	$\tilde{N}$	E_g	E'_g	E''_g	MC	MP
Sc	7.595	9.566	-427.68	-6.31	1.59	-2.93	2.07	2.16[a]		0.48	0.28
Y	7.611	9.667	-426.66	-6.45	2.74	-3.08	2.03	2.13[b]	2.14[g]	0.49	0.26
La	7.593	9.889	-423.93	-4.85	3.88	-3.09	1.97			0.58	0.14
TiO_2	7.564	9.564	-430.85	-7.90	0.00	-3.28	3.18	3.14[c]		0.67	0.38
Zr	7.594	9.622	-431.75	-8.56	-0.23	-3.07	2.06	2.23[b]	2.33[h]	0.69	0.30
Hf	7.589	9.608	-434.02	-9.96	-1.10	-3.11	2.09			0.66	0.40
V	7.562	9.533	-429.49	-9.07	2.54	-5.61	1.90	1.71,[d] 1.82[b]	2.23[i]	0.86	0.20
Nb	7.598	9.556	-431.26	-10.09	1.79	-5.70	2.09	2.07,[e] 2.18[f]	2.20[j]	0.79	0.39
Ta	7.598	9.551	-434.20	-11.85	0.61	-5.73	2.17			0.74	0.48

[a] Reference [47]

[b] Reference [48]

[c] Reference [46]

[d] Reference [19]

[e] Reference [45]

[f] Reference [44]

[g] Reference [52]

[h] Reference [51]

[i] Reference [50]

[j] Reference [49]

Fig. 1

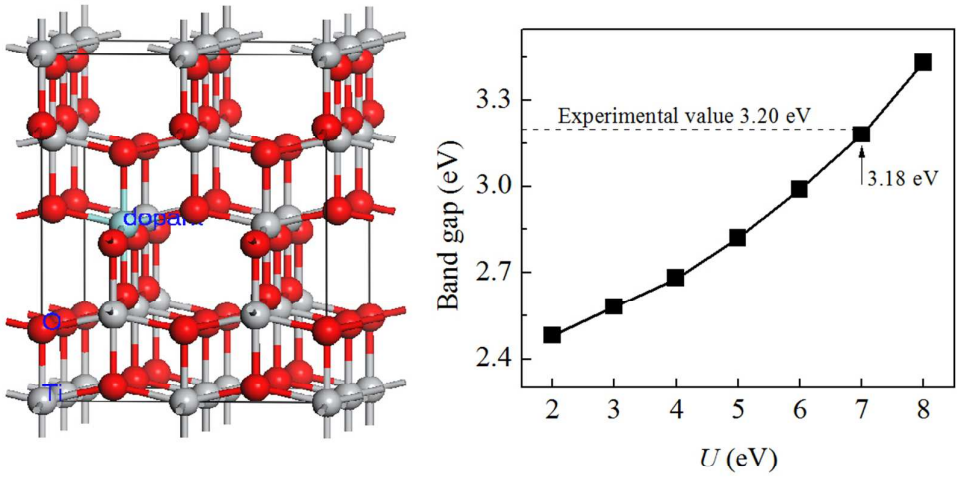

(a) (b)

Fig. 2

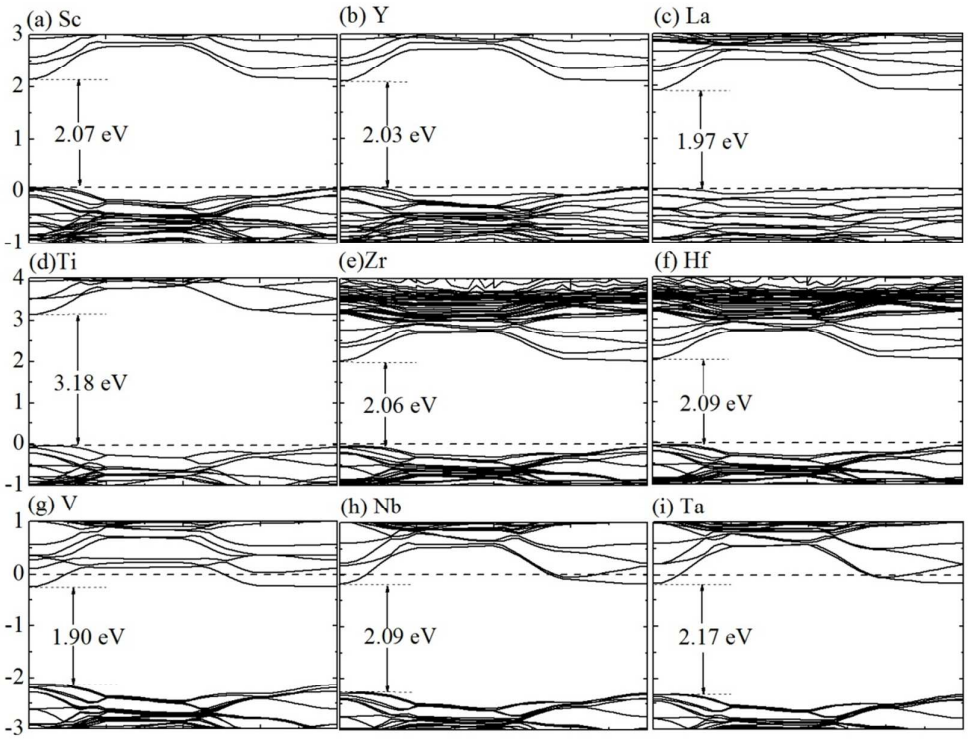

Fig. 3

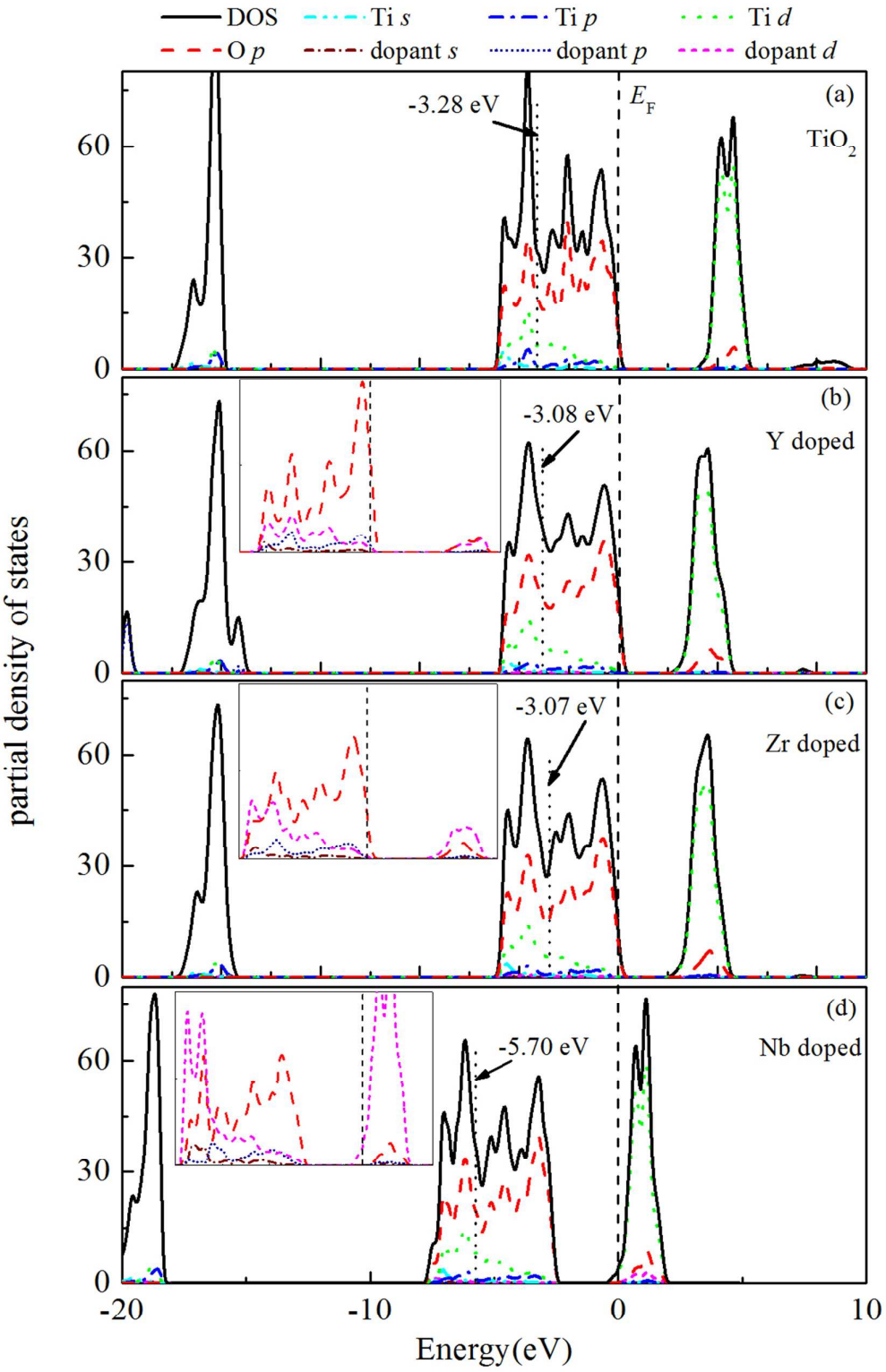

Fig. 4